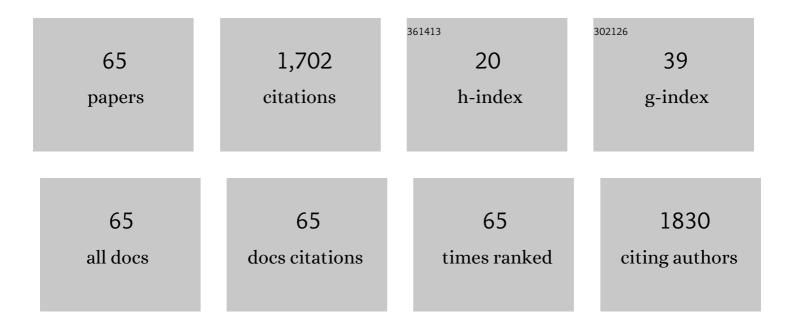
## Ning Wang

List of Publications by Year in descending order

Source: https://exaly.com/author-pdf/9579056/publications.pdf Version: 2024-02-01



#	Article	IF	CITATIONS
1	Effect of the NiN2S2 Metallothiolate Ligands on the Preparation, Structure, and Property of Dinickel Complexes Related to [NiFe]-Hydrogenases Active Site. Catalysis Letters, 2022, 152, 98-105.	2.6	0
2	A zinc porphyrin polymer as efficient bifunctional catalyst for conversion of CO <sub>2</sub> to cyclic carbonates. Applied Organometallic Chemistry, 2022, 36, .	3.5	10
3	Sensitive and precise visually guided drug delivery nanoplatform with dual activation of pH and light. Acta Biomaterialia, 2022, 141, 374-387.	8.3	9
4	Zinc(II)porphyrin-Based Porous Ionic Polymers (PIPs) as Multifunctional Heterogeneous Catalysts for the Conversion of CO <sub>2</sub> to Cyclic Carbonates. Industrial & Engineering Chemistry Research, 2022, 61, 5093-5102.	3.7	16
5	Covalent Metalloporphyrin Polymer Coated on Carbon Nanotubes as Bifunctional Electrocatalysts for Water Splitting. Inorganic Chemistry, 2022, 61, 10198-10204.	4.0	11
6	Molecular Cobalt Catalysts Grafted onto Polymers for Efficient Hydrogen Generation Cathodes. Solar Rrl, 2021, 5, 2000281.	5.8	3
7	Triple-responsive targeted hybrid liposomes with high MRI performance for tumor diagnosis and therapy. Materials Chemistry Frontiers, 2021, 5, 6226-6243.	5.9	5
8	Endogenous reactive oxygen species burst induced and spatiotemporally controlled multiple drug release by traceable nanoparticles for enhancing antitumor efficacy. Biomaterials Science, 2021, 9, 4968-4983.	5.4	10
9	Photo(electro)catalytic activity enhancement of PhC <sub>2</sub> Cu by Fe doping induced energy band modulation and luminescence chromism switching. Catalysis Science and Technology, 2021, 11, 2379-2385.	4.1	10
10	Electrostatic Interactions Accelerating Water Oxidation Catalysis via Intercatalyst O–O Coupling. Journal of the American Chemical Society, 2021, 143, 2484-2490.	13.7	25
11	Engineering heterostructure and crystallinity of Ru/RuS2 nanoparticle composited with N-doped graphene as electrocatalysts for alkaline hydrogen evolution. Chinese Chemical Letters, 2021, 32, 3591-3595.	9.0	16
12	Synthesis of Mn (III)–porphyrin porous coordination polymers as heterogeneous catalysts for CO 2 cycloaddition reaction. Applied Organometallic Chemistry, 2021, 35, e6228.	3.5	4
13	A Traceable, Sequential Multistageâ€Targeting Nanoparticles Combining Chemo/Chemodynamic Therapy for Enhancing Antitumor Efficacy. Advanced Functional Materials, 2021, 31, 2101432.	14.9	24
14	A traceable, GSH/pH dual-responsive nanoparticles with spatiotemporally controlled multiple drugs release ability to enhance antitumor efficacy. Colloids and Surfaces B: Biointerfaces, 2021, 205, 111866.	5.0	14
15	Introducing electrostatic interaction into Ru(bda) complexes for promoting water-oxidation catalysis. Journal of Molecular Structure, 2021, 1242, 130745.	3.6	1
16	An MRI-guided targeting dual-responsive drug delivery system for liver cancer therapy. Journal of Colloid and Interface Science, 2021, 603, 783-798.	9.4	10
17	Magnetic Resonance Imaging-Guided Multi-Stimulus-Responsive Drug Delivery Strategy for Personalized and Precise Cancer Treatment. ACS Applied Materials & Interfaces, 2021, 13, 50716-50732.	8.0	9
18	Precise delivery of multi-stimulus-responsive nanocarriers based on interchangeable visual guidance. Materials Science and Engineering C, 2021, , 112558.	7.3	5

#	Article	IF	CITATIONS
19	Meshless Method for Nonuniform Heat-Transfer/Solidification Behavior of Continuous Casting Round Billet. Metallurgical and Materials Transactions B: Process Metallurgy and Materials Processing Science, 2020, 51, 236-246.	2.1	6
20	Orthogonal Supramolecular Assembly Triggered by Inclusion and Exclusion Interactions with Cucurbit[7]uril for Photocatalytic H 2 Evolution. ChemSusChem, 2020, 13, 394-399.	6.8	13
21	Pyridiniumâ€functionalized metalloporphyrins as bifunctional catalysts for cycloaddition of epoxides and carbon dioxide. Applied Organometallic Chemistry, 2020, 34, e5382.	3.5	11
22	A Multifunctional Lipid Incorporating Active Targeting and Dual-Control Release Capabilities for Precision Drug Delivery. ACS Applied Materials & amp; Interfaces, 2020, 12, 70-85.	8.0	21
23	Ultrasmall Ru Nanoparticles Highly Dispersed on Sulfur-Doped Graphene for HER with High Electrocatalytic Performance. ACS Applied Materials & Interfaces, 2020, 12, 48591-48597.	8.0	87
24	Ru/RuO <sub>2</sub> Nanoparticle Composites with N-Doped Reduced Graphene Oxide as Electrocatalysts for Hydrogen and Oxygen Evolution. ACS Applied Nano Materials, 2020, 3, 12269-12277.	5.0	68
25	Bioinspired Design of Positioned Amine Assists Hydrogen Evolution from Neutral Water by Nickel Tripyridineâ€Điamine. ChemCatChem, 2020, 12, 3853-3856.	3.7	1
26	Cycloaddition Reactions of Epoxides and CO <sub>2</sub> by the Novel Imidazoliumâ€Functionalized Metalloporphyrins: Optimization and Analysis using Response Surface Methodology. ChemCatChem, 2020, 12, 4839-4844.	3.7	13
27	Synthesis, structure and electrocatalytic H2-evoluting activity of a dinickel model complex related to the active site of [NiFe]-hydrogenases. Chinese Chemical Letters, 2020, 31, 2483-2486.	9.0	4
28	Efficient antibacterial dextran-montmorillonite composite sponge for rapid hemostasis with wound healing. International Journal of Biological Macromolecules, 2020, 160, 1130-1143.	7.5	40
29	A multifunctional lipid that forms contrast-agent liposomes with dual-control release capabilities for precise MRI-guided drug delivery. Biomaterials, 2019, 221, 119412.	11.4	53
30	Metalloporphyrinsâ€Al <sup>3+</sup> porous coordination polymers: Preparations, Characterizations and Catalytic Properties. Applied Organometallic Chemistry, 2019, 33, e5055.	3.5	3
31	Study of factors influencing the fabrication of Coâ€porphyrin porous coordination polymer via metal–organic gel intermediate. Applied Organometallic Chemistry, 2019, 33, e5215.	3.5	1
32	Photocatalytic Hydrogen Production Based on a Serial Metalâ€Salen Complexes and the Reaction Mechanism. ChemCatChem, 2019, 11, 6324-6331.	3.7	25
33	A highly efficient, in situ wet-adhesive dextran derivative sponge for rapid hemostasis. Biomaterials, 2019, 205, 23-37.	11.4	160
34	Synthesis and evaluation of mono- and multi-hydroxyl low toxicity pH-sensitive cationic lipids for drug delivery. European Journal of Pharmaceutical Sciences, 2019, 133, 69-78.	4.0	9
35	Current progress in interfacial engineering of carbon-based perovskite solar cells. Journal of Materials Chemistry A, 2019, 7, 8690-8699.	10.3	84
36	Effective wound dressing based on Poly (vinyl alcohol)/Dextran-aldehyde composite hydrogel. International Journal of Biological Macromolecules, 2019, 132, 1098-1105.	7.5	58

#	Article	IF	CITATIONS
37	Synthesis and characterization of porphyrin-based porous coordination polymers obtained by supercritical CO2 extraction. Journal of Materials Science, 2018, 53, 10534-10542.	3.7	9
38	Preparation, characterization and catalytic oxidation properties of silica composites immobilized with cationic metalloporphyrins. Journal of Materials Science, 2018, 53, 14241-14249.	3.7	6
39	Seamless Interfacial Formation by Solution-Processed Amorphous Hydroxide Semiconductor for Highly Efficient Electron Transport. ACS Applied Energy Materials, 2018, 1, 4564-4571.	5.1	16
40	Complexes of MN <sub>2</sub> S <sub>2</sub> ·Fe(η <sup>5</sup> -C <sub>5</sub> R <sub>5</sub> )(CO) as platform for exploring cooperative heterobimetallic effects in HER electrocatalysis. Dalton Transactions, 2017, 46, 5617-5624.	3.3	24
41	Halideâ€Anion Water Clusters in Cucurbit[6]uril Supramolecular Systems. Chinese Journal of Chemistry, 2016, 34, 1114-1120.	4.9	4
42	Cyanide-bridged iron complexes as biomimetics of tri-iron arrangements in maturases of the H cluster of the di-iron hydrogenase. Chemical Science, 2016, 7, 3710-3719.	7.4	20
43	Using a novel adsorbent macrocyclic compound cucurbit[8]uril for Pb 2+ removal from aqueous solution. Journal of Environmental Sciences, 2016, 50, 3-12.	6.1	19
44	Hemilabile Bridging Thiolates as Proton Shuttles in Bioinspired H <sub>2</sub> Production Electrocatalysts. Journal of the American Chemical Society, 2016, 138, 12920-12927.	13.7	78
45	Effect of Bridgehead Steric Bulk on the Intramolecular C–H Heterolysis of [FeFe]-Hydrogenase Active Site Models Containing a P <sub>2</sub> N <sub>2</sub> Pendant Amine Ligand. Inorganic Chemistry, 2016, 55, 411-418.	4.0	17
46	The influence of a S-to-S bridge in diiron dithiolate models on the oxidation reaction: a mimic of the Hairox state of [FeFe]-hydrogenases. Chemical Communications, 2014, 50, 9255-9258.	4.1	15
47	Redox Reactions of [FeFe]-Hydrogenase Models Containing an Internal Amine and a Pendant Phosphine. Inorganic Chemistry, 2014, 53, 1555-1561.	4.0	24
48	Intramolecular Iron-Mediated C–H Bond Heterolysis with an Assist of Pendant Base in a [FeFe]-Hydrogenase Model. Journal of the American Chemical Society, 2014, 136, 16817-16823.	13.7	38
49	Reactions of [FeFe]-hydrogenase models involving the formation of hydrides related to proton reduction and hydrogen oxidation. Dalton Transactions, 2013, 42, 12059.	3.3	104
50	Modeling of capacitively coupled contactless conductivity detection on microfluidic chips. Microsystem Technologies, 2013, 19, 1991-1996.	2.0	3
51	Catalytic Activation of H <sub>2</sub> under Mild Conditions by an [FeFe]-Hydrogenase Model via an Active μ-Hydride Species. Journal of the American Chemical Society, 2013, 135, 13688-13691.	13.7	107
52	Chloridobis(dimethylglyoximato-κ2N,N′)(ethyl pyridine-3-carboxylate-κN)cobalt(III). Acta Crystallographica Section E: Structure Reports Online, 2012, 68, m20-m20.	0.2	0
53	Chloridobis(dimethylglyoximato-κ2N,N′)(ethyl pyridine-4-carboxylate-κN)cobalt(III) chloroform monosolvate. Acta Crystallographica Section E: Structure Reports Online, 2012, 68, m204-m205.	0.2	1
54	Pseudopolyrotaxanes of Cucurbit[6]uril: A Threeâ€Dimensional Network Selfâ€assembled by ClO <sub>4</sub> <sup>â^'</sup> (H <sub>2</sub> O) <sub>2</sub> Water Clusters. Chinese Journal of Chemistry, 2012, 30, 941-946.	4.9	9

#	Article	IF	CITATIONS
55	The antimicrobial activities of a series of bis-quaternary ammonium compounds. Chinese Chemical Letters, 2011, 22, 887-890.	9.0	14
56	Synthesis, protonation and electrochemical properties of trinuclear NiFe2 complexes Fe2(CO)6(l¼3-S)2[Ni(Ph2PCH2)2NR] (R=n-Bu, Ph) with an internal pendant nitrogen base as a proton relay. Inorganica Chimica Acta, 2009, 362, 372-376.	2.4	14
57	Protophilicity, electrochemical property, and desulfurization of diiron dithiolate complexes containing a functionalized C2 bridge with two vicinal basic sites. Polyhedron, 2009, 28, 1138-1144.	2.2	8
58	Preparation, Facile Deprotonation, and Rapid H/D Exchange of the μ-Hydride Diiron Model Complexes of the [FeFe]-Hydrogenase Containing a Pendant Amine in a Chelating Diphosphine Ligand. Inorganic Chemistry, 2009, 48, 11551-11558.	4.0	84
59	[FeFe]-Hydrogenase active site models with relatively low reduction potentials: Diiron dithiolate complexes containing rigid bridges. Journal of Inorganic Biochemistry, 2008, 102, 952-959.	3.5	16
60	A proton–hydride diiron complex with a base-containing diphosphine ligand relevant to the [FeFe]-hydrogenase active site. Chemical Communications, 2008, , 5800.	4.1	73
61	Supramolecular self-assembly of a [2Fe2S] complex with a hydrophilic phosphine ligand. CrystEngComm, 2008, 10, 267-269.	2.6	18
62	CO-Migration in the Ligand Substitution Process of the Chelating Diphosphite Diiron Complex (μ-pdt)[Fe(CO) <sub>3</sub> ][Fe(CO){(EtO) <sub>2</sub> PN(Me)P(OEt) <sub>2</sub> }]. Inorganic Chemistry, 2008, 47, 6948-6955.	4.0	50
63	Carbene–pyridine chelating 2Fe2S hydrogenase model complexes as highly active catalysts for the electrochemical reduction of protons from weak acid (HOAc). Dalton Transactions, 2007, , 1277-1283.	3.3	85
64	Polydopamine Decorated Ru-Ni(OH)2 Nanosheets for Enhanced Performance of Hydrogen Evolution in Alkaline Media. Catalysis Letters, 0, , 1.	2.6	1
65	A Benzimidazoleâ€linked Porphyrin Covalent Organic Polymers as Efficient Heterogeneous Catalyst/Photocatalyst. Applied Organometallic Chemistry, 0, , .	3.5	6